Crystal structure of the C-terminal SH2 domain of the p85a regulatory subunit of phosphoinositide 3-kinase: a SH2 domain mimicking its own substrate

Hoedemaeker, F.J.; Siegal, G.D.; Roe, S.M.; Driscoll, P.C.; Abrahams, J.P.

Article No. jmbi.1999.3111 available online at http://www.idealibrary.com on IDEAL® J. Mol. Biol. (1999) 292, 763–770

JMB

COMMUNICATION

Crystal Structure of the C-Terminal SH2 Domain of the p85α Regulatory Subunit of Phosphoinositide 3-Kinase: An SH2 Domain Mimicking its Own Substrate

Flip J. Hoedemaeker[1]*, Gregg Siegal[1], S. Mark Roe[2,3], Paul C. Driscoll[2,3] and Jan Pieter Abrahams[1]

[1]*Leiden Institute for Chemistry Gorlaeus Laboratoria Universiteit Leiden postbus 9502, 2300 RA, Leiden The Netherlands*

[2]*Department of Biochemistry and Molecular Biology University College London Gower Street, London WC1E 6BT, UK*

[3]*Ludwig Institute for Cancer Research, 91 Riding House St London WC1P 8BT, UK*

**Corresponding author*

The binding properties of Src homology-2 (SH2) domains to phosphotyrosine (pY)-containing peptides have been studied in recent years with the elucidation of a large number of crystal and solution structures. Taken together, these structures suggest a general mode of binding of pY-containing peptides, explain the specificities of different SH2 domains, and may be used to design inhibitors of pY binding by SH2 domain-containing proteins. We now report the crystal structure to 1.8 Å resolution of the C-terminal SH2 domain (C-SH2) of the P85α regulatory subunit of phosphoinositide 3-kinase (PI3 K). Surprisingly, the carboxylate group of Asp2 from a neighbouring molecule occupies the phosphotyrosine binding site and interacts with Arg18 (αA2) and Arg36 (βB5), in a similar manner to the phosphotyrosine-protein interactions seen in structures of other SH2 domains complexed with pY peptides. It is the first example of a non-phosphate-containing, non-aromatic mimetic of phosphotyrosine binding to SH2 domains, and this could have implications for the design of substrate analogues and inhibitors. Overall, the crystal structure closely resembles the solution structure, but a number of loops which demonstrate mobility in solution are well defined by the crystal packing. C-SH2 has adopted a binding conformation reminiscent of the ligand bound N-terminal SH2 domain of PI3K, apparently induced by the substrate mimicking of a neighbouring molecule in the crystal.

Keywords: inhibitor; SH2; PI3K; phosphotyrosine mimic; structure-aided design

Background

Src homology-2 (SH2) domains are protein modules of approximately 100 residues that bind to proteins containing phosphotyrosine (pY) in the context of short, well-characterised motifs (Songyang *et al.*, 1993). The SH2 domain-containing class IA phosphoinositide 3-kinase (PI3K) is an important second messenger generator that has been implicated in many intracellular signalling pathways, including growth factor-induced mitogenic responses (Toker & Cantley, 1997; Vanhaesebroeck *et al.*, 1997). Phosphoinositide 3-kinases belonging to this class and which are regulated by growth factor receptor tyrosine kinases, are tightly coupled heterodimers consisting of an 85 kDa regulatory subunit (p85) and a 110 kDa catalytic subunit (p110). The p85 subunit consists of a Src homology-3 (SH3) domain, a BCR/Rho GAP homology domain, an SH2 domain (N-SH2), a ca 200 residue region involved in the interaction with the p110 subunit, and a second SH2 domain (C-SH2) (Otsu *et al.*, 1991; Dhand *et al.*, 1994). The two SH2 domains of p85 recognise similar consensus pY motifs with the sequence pattern pY-Val/Met-X-Met in the activated PDGF receptor, pY740 and pY751 (Songyang *et al.*, 1993; Kashishian *et al.*, 1992; Panayotou *et al.*, 1993; Rordorf-Nikolic *et al.*, 1995). It has been postulated that C-SH2 binds the

Abbreviations used: SH2, Src homology-2; pY, phosphotyrosine; PI3K, phosphoinositide 3-kinase; SH3, Src homology-3 C-SH2, C-terminal SH2 domain; N-SH2, N-terminal SH2 domain.

E-mail address of the corresponding author: hoedemae@chem.leidenuniv.nl

0022-2836/99/390763–8 $30.00/0

pY740 site and N-SH2 the pY751 site (Siegal *et al.*, 1998).

Over the past few years a number of high-resolution three-dimensional structures of SH2 domains, both in the presence and the absence of their phosphotyrosine peptide ligands, have been obtained. At present, the protein database contains 12 crystal structures of SH2 domains with a resolution of 2 Å or better, and 14 NMR structures (Abola *et al.*, 1997). Figure 1 shows a sequence alignment based on the 3D structure of a subset of SH2 domains whose high-resolution X-ray structures or NMR solution structures have previously been determined. The polypeptide fold of the SH2 domains is highly conserved and primarily consists of a central three-stranded β-sheet comprising β-strands βB, βC and βD, flanked by conserved α-helices αA and αB (Figure 2), according to the nomenclature described by Eck *et al.* (1993). The basis for the recognition of high-affinity pY peptides by SH2 domains was revealed by a number of NMR and X-ray structures of SH2 domain-peptide complexes (Waksman *et al.*, 1993; Eck *et al.*, 1993; Pascal *et al.*, 1994). In what has been termed the ''plug and socket'' mechanism, side-chains of the pY peptide at positions pY, pY + 1 and pY + 3 are directed into binding pockets on either side of the central β-sheet. The most strongly conserved interaction between the SH2 domain and the peptide ligand occurs at the pY-binding site with the guanidinium group of the invariant arginine residue at position βB5 (Waksman *et al.*, 1993) directly ligating the oxygen atoms of the anionic pY phosphate group. Additional interactions include the side-chains of a second arginine residue (αA2) and a serine residue (βB7), but these interactions are less strictly conserved. The binding pocket for pY + 1 and pY + 3 provides additional binding specificity of the SH2 domain for particular pY-peptide sequence motifs. The residue at position βD5 (Cys 57 in C-SH2) plays an important role in determining the ligand binding specificity at both the pY + 1 and pY + 3 positions (Songyang *et al.*, 1995; Siegal *et al.*, 1998). Whilst the side-chain of residue βD5 has been recognised to play a significant role in determining the ligand specificity, the precise selection of residue type in each of the pY + 1 and pY + 3 positions is not readily explained.

Structure-based design of substrate analogues and inhibitors of SH2 domains has been initiated in a number of research groups in recent years (Groves *et al.*, 1998; Fu & Castelhano, 1998; Yao *et al.*, 1999). Ongoing structural studies are still required for a better understanding of the mode of interaction of these proteins with various ligands. Of particular interest is the interaction of SH2 domains with compounds other than pY peptides. Here we present the crystal structure of C-SH2 at 1.8 Å resolution. The crystal structure reveals a surprising interaction at the pY binding site with implications for the design of non-pY and non-peptide SH2 inhibitors.

Crystal formation and structure elucidation

Crystals of C-SH2 were obtained serendipitously from a sample prepared for NMR (50 mM Tris-HCl (pH 7.5), 50 mM NaCl, 1 mM EDTA, 1 mM DTT, 1 mM protein (~13 mg/ml) at 4 °C). Later attempts to crystallise C-SH2 from this particular solution only resulted in micro-crystals of non-defracting quality. A data set from a single crystal was taken at the Daresbury synchrotron source, consisting of 45 frames with 2° oscillations at 100 K. Data were indexed with Mosflm and scaled with Scala (CCP4, 1994; Evans, 1997). C-SH2 crystallised in the $P2_12_12_1$ space group with unit cell dimensions of $x = 38.68$ Å, $y = 46.92$ Å and $z = 62.98$ Å. Previously, it has proven difficult to solve SH2 domain structures using molecular replacement techniques (Nolte *et al.*, 1996). However, we were able to obtain a solution with the ensemble of 30 NMR-derived conformers using a ''brute force'' approach. Once satisfactory translation and rotation functions were found, phases

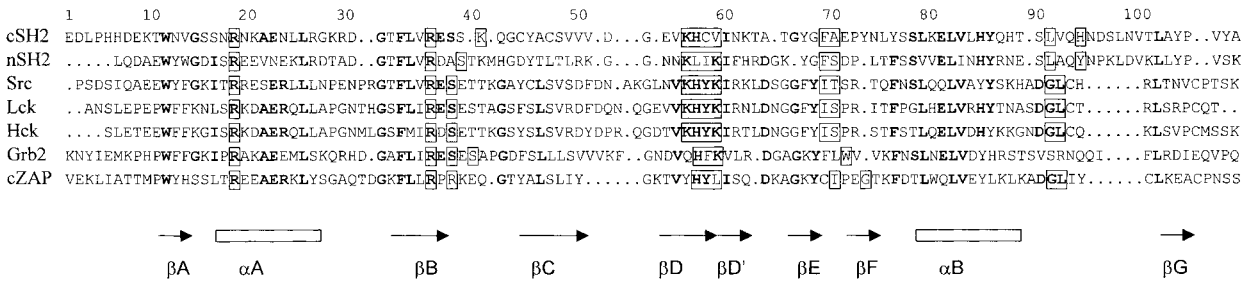

Figure 1. Structural alignment of several SH2 domains. The nomenclature of the secondary structure elements is given underneath the sequence. Residues involved in ligand binding are boxed, conserved residues are printed in bold. Abbreviations: C-SH2, C-terminal SH2 domain of PI3K p85α (this study); N-SH2, N-terminal SH2 domain of PI3 K p85α (Nolte *et al.*, 1996); Src, SH2 domain from Src tyrosine kinase (Waksman *et al.*, 1993); Lck, the SH2 domain of p56ck (Mikol *et al.*, 1995); Hck, SH2 domain of hematopoietic cellular kinase (Zhang *et al.*, l997); Grb2, SH2 domain of Grb2 adapter protein (Rahuel *et al.*, 1996); cZAP, SH2 domain of ZAP-70 protein tyrosine kinase (Hatada *et al.*, 1995).

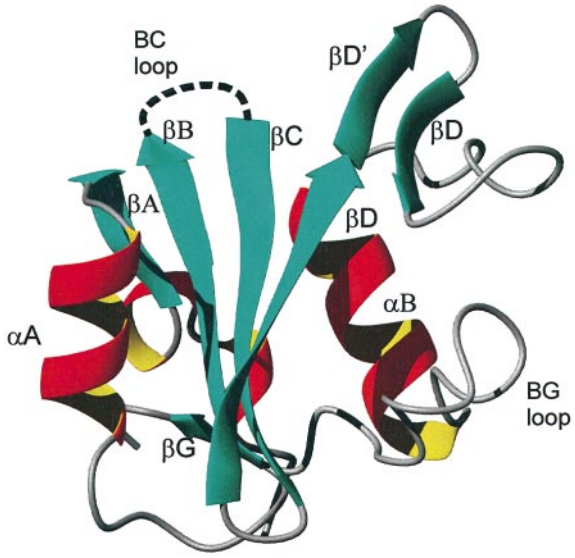

Figure 2. Ribbon diagram of the crystal structure of C-SH2. The various structural elements are labelled using the nomenclature described by Eck *et al*. (1993). The disordered BC loop (residues 39-42) is indicated with a broken line.

were improved using unrestrained refinement with the new ''autobuilding'' module in wARP (Perrakis *et al*., 1999). In the end the structure was refined using data to 1.8 Å with an R_{free} of 23.6 % (see Table 1).

Structure comparison

Here we compare the present crystal structure of C-SH2 with the solution structure of the same molecule both free (PDB entry code 1BFJ) and in complex with a peptide derived from the pY751 site of the PDGF receptor (PDB entry code 1PIC). In order to gain additional insight into the ligand protein interaction, we compare the present structure with the crystal structures of the N-terminal SH2 domain of p85α (N-SH2), both free and with bound pY peptides (Nolte, 1996; PDB codes not deposited). We will refer to the pY peptide TNEpYMDMK derived from c-kit Y721 as simply pY-c-kit and the pY peptide SIDpYVPMLDMK derived from PGDF receptor Y719 as pY-PDGFR.

Figure 3 shows a superposition using the conserved secondary structure elements of the crystal structure and the ensemble of NMR conformers of C-SH2. As expected, the structures are quite similar with an RMSD of 0.92 Å to the energy-minimised mean NMR structure for all C^{α} atoms in non-loop regions (residues 11-14, 19-24, 32-37, 43-50, 53-59, 78-86, 103-105). There are, however, significant differences in the orientation of helix αA and the BC loop. Helix αA forms part of the pY binding site and we focus on this region first.

Table 1. Data collection, structure determination and refinement statistics

	23-1.8 Å	1.85-1.80 Å
Total reflections	37,237	2058
Unique reflections	10,984	677
R_{meas} (%)	4.4	6.8
I/σ	7.2	10.2
Multiplicity	3.4	3.0
Completeness (%)	98.7	84.5
Final refinement statistics		
	123-1.80 Å	11.89-1.80 Å
R-factor (%)	15.8	11.8
No. refl. working set	9826	1159
R_{free} (%)	23.6	23.1
No. refl. test set	1121	135
RMS deviation bond lengths (Å)		0.008
RMS deviation bond angles (deg.)		2.10
Overall coordinate ESU based on R_{free} (Å)		0.14
Overall coordinate ESU based on ML (Å)		0.08
Average *B*-value protein (832 atoms)(Å^2)		19.2
Average *B*-value main-chain atoms (Å^2)		17.5
Average *B*-value side-chain atoms (Å^2)		20.9
Average *B*-value water (185 water molecules) (Å^2)		35.7

An MR model was found using a brute force approach, translational searches were done in AMoRe (CCP4, 1994) for all rotations of each of the NMR solution conformers in increments of 5°, followed by rigid body refinement. The final MR solution was generated from several NMR structures after several rounds of simulated annealing in X-PLOR (Brünger, 1992) and careful interpretation of generated electron density maps. This model was used as a starting point for extensive unrestrained refinement, using the new Auto-tracing option in ARP/wARP version 5.0 (Perrakis *et al*., 1999), in combination with manual rebuilding in O (Jones *et al*., 1991). Eventually, 97 out of 111 residues were traced with a connectivity index of 0.94. In the map generated from this model the protein could be traced completely, with the exception of three residues in the BC loop (residues 39-41) and the final four residues of the C terminus (residues 108-111). Final refinement was done with Refmac (Murshudov *et al*., 1997) and wARP with anisotropic bulk solvent correction. All reflections measured were used in refinement. In the last refinement round anisotropic *B*-values were refined. After refinement the model was checked for errors using WHAT_CHECK (Hooft *et al*., 1996).

pY binding site

A most surprising aspect of the crystal structure determination was the discovery that Asp2, which is completely disordered in solution (Siegal *et al*., 1998; Kristensen *et al*., unpublished results), occupies the phosphotyrosine binding site of a neighbouring molecule in a manner highly reminiscent of structures of SH2-pY peptide complexes (Figure 4(a) and (c)). The residues normally involved in pY binding, Arg18 (αA2) and Arg36 (βB5) (Figure 1), form intermolecular salt bridges to the carboxylate group of Asp2 (Figure 4(a)). Interestingly, the interatomic O to O distance is very similar in carboxylate and phosphate groups, thus allowing nearly perfect, simultaneous interaction of both guanidinium nitrogen atoms of Arg36 (βB5) with the side-chain oxygen atoms of

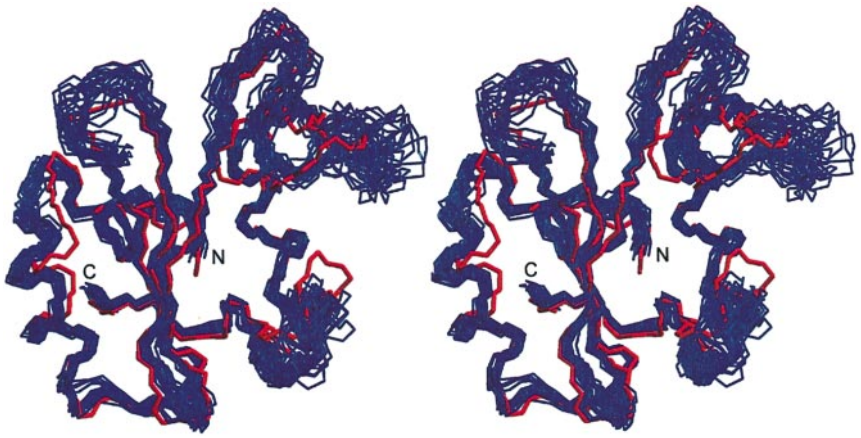

Figure 3. Stereo image of the superposition of the ensemble of NMR conformers and the crystal structure of C-SH2. The backbone of the crystal structure is shown in red, while that of the NMR conformers is shown in blue. The N and C termini are marked. The disordered BC loop (residues 39-42) is replaced by a pseudobond between C′ of residue 38 and N of residue 43. The superposition was based on the backbone atoms of residues 11-14, 19-24, 32-37, 43-50, 53-59, 78-86, 103-105.

Asp2 (N-O distances 2.9 and 2.8 Å). The absence of the bulky phenyl ring allows an unusually close approach of the Arg18 (αA2) $N^{\eta 1}$ atom to the Asp2 $O^{\delta 2}$ atom (2.8 Å). This is the first experimentally based structure in which a non-phenyl ring-containing compound is seen bound in the phosphotyrosine binding pocket of an SH2 domain. This observation possibly opens the way towards design of a new class of SH2 domain inhibitors that do not contain a phenyl ring. Interestingly, the isolated C-SH2 domain has a high tendency to form aggregates in solution, as seen in dynamic light-scattering experiments and NMR relaxation times (data not shown). The tendency to aggregate is diminished by the addition of pY peptides. This fact implies that the interaction seen in the crystal may also be present in solution, albeit weakly.

The binding of Asp2 in the pY pocket results in important differences between the solution and crystal structures of C-SH2. First, the side-chains of Arg18 (αA2) and Arg36 (βB5) are well defined in the crystal structure (mean isotropic *B*-values are 18.5 and 13.9 $Å^2$, respectively), whereas their local displacements are greater than average in solution (Siegal *et al.*, 1998). The Asp2 side-chain binds to the pY binding pocket from a different angle and in a different peptide backbone context than observed for pY peptide ligands, demonstrating the adaptability of the pY binding pocket. The interaction is stabilised by a number of well-ordered water molecules, especially in the vicinity of Arg36 (see Figure 4(b)). In solution, Arg18 (αA2) is solvent exposed and therefore has few steric constraints. In the crystal, Arg18 (αA2) takes part in additional stacking interactions with His56 (βD4) and with His6 (αN) from the same neighbouring molecule (Figure 4(a)). Yet another intermolecular hydrogen bond is formed between Asn17 (αA1) and E70 (βF1) of a second crystallographic neighbour, although this interaction does not appear to have a physiological relevance. It is likely that these three interactions (pY site binding, stacking and intermolecular hydrogen bonding) serve to lock helix αA into one conformation resulting in the low *B*-values. By comparison, the conformation of helix αA is not as well defined by the NMR data. It is also likely that these three interactions force helix αA closer to the central β-sheet than in the NMR solution structure of either the ligand-free or ligand-bound forms of C-SH2. Superposition of the crystal structure of C-SH2 with that of the ligand-free N-SH2 results in an RMSD of 0.89 Å for all C^{α} atoms in non-loop regions (residues 11-14, 19-24, 32-37, 43-50, 53-59, 78-86, 103-105). Here again helix αA lies closer to the central β-sheet in C-SH2 than in N-SH2. The stacking and intermolecular hydrogen bonds seen in the crystal structure of C-SH2 are not present in N-SH2. Probably due to the pY mimicking function of the neighbouring Asp2, the side-chain of C-SH2 Arg18 (αA2) faces into the pY pocket placing it in a conformation closer to that of Arg19 (αA2) in the ligand-bound N-SH2 than in the ligand-free form.

BC loop

The BC loop also contributes residues towards ligation of pY, however their precise nature and location in the primary structure differs from one SH2 domain to the next (Figure 1). We have previously shown by mutagenesis that residues Ser38 (βB7), Ser39 (BC1) and Lys40 (BC2) are increasingly important for binding of target pY peptides (Siegal *et al.*, 1998). In the solution structure of C-SH2 we noted that the BC loop was poorly defined by the NMR data. Recently we have shown that this loop undergoes fast dynamic behaviour as well as conformational exchange (Kristensen *et al.*, unpublished results). The BC loop in the present crystal structure is mostly disordered. No interpretable density was found for residues Ser39 (BC1), Lys40 (BC2), and Gln41 (BC3). Therefore, determination of the conformation of this loop and how it interacts with the pY residue awaits further experimentation.

βD strand

In the crystal structure, the side-chain of His56 (βD4) makes a hydrogen bond with Glu22 (αA6).

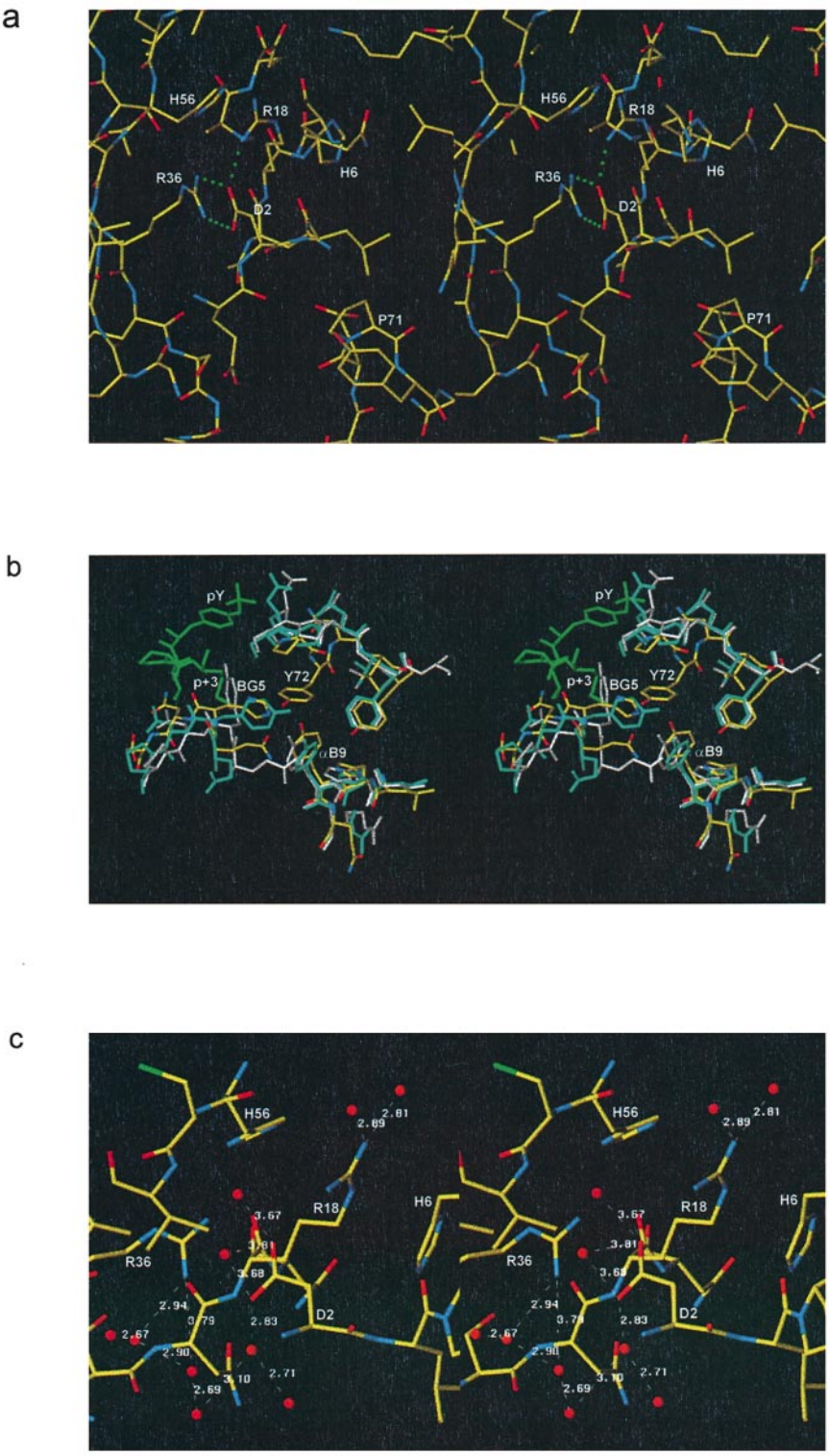

Figure 4. Detailed (divergent) stereo images. (a) The binding of Asp2 of a crystallographic neighbour to the active-site residues Arg18 (αA2) and Arg36 (βB5). Pro71 of a third SH2 molecule is also involved in this crystal contact. (b) Water structure surrounding the binding pocket: a network of well-ordered water molecules forms one side of the binding pocket. (c) The binding pocket for the ligand residue Met pY + 3. Ligand-free N-SH2 is shown in grey, N-SH2 liganded to pY-PDGFR is shown in blue (with part of the pY peptide in green), and C-SH2 is shown in CPK colouring. His BG6 is in a position comparable with liganded N-SH2 and not with unliganded N-SH2, making a hydrogen bond to Tyr αB9. The insertion of Tyr72 in the sequence is clearly visible.

This interaction is not seen in the NMR structure of the ligand-free C-SH2, where the carboxylate group of Glu22 (αA6) faces into the solution. However, the hydrogen bond is seen in the energy-minimised, mean structure of the C-SH2-pY751 complex (Breeze *et al.*, 1996). This interaction looks to be incompatible with the binding of the pY-2 residue (Asn) as seen in the crystal structure of N-SH2 with pY-c-kit (data not shown). As the peptide chosen for the solution studies did not include the $i-2$ residue, conformation of this hypothesis must await further efforts.

βE and βF, EF loop

In the solution structure of the ligand-free C-SH2, the entire region from residue Asn60 (βD′2) to Ser76 (FG2) is poorly ordered (Figure 3). We proposed that this region is involved in either dynamic behaviour on the intermediate (millisecond) time-scale and/or conformational exchange processes in solution (Siegal *et al.*, 1998). Recent work confirms this hypothesis (Kristensen *et al.*, unpublished results). However, in our present crystal structure, this region is well defined with *B*-factors typical of the protein as a whole (on average 19.2 Å^2). Two important crystal contacts appear to contribute to the ''locking in'' of the conformation of this region. First, residues Ala69 (EF1) through Tyr75 (FG1) form a protuberance from the surface of C-SH2. In the crystal structure, this region primarily packs tightly against exposed hydrophobic residues in helix αB of a neighbouring molecule. A second crystal contact is made by Glu70 (EF2), which forms an intermolecular hydrogen bond to Asn 17 (αA1) of a second neighbour. Another important contribution to the conformation of this region seems to be the docking of the side-chain of Phe68 (βE4). In the crystal structure, the phenyl ring of Phe68 is tucked into the core of the protein forming the ''roof'' of a hydrophobic binding pocket for the $pY+1$ and $pY+3$ ligand residues. In contrast, Phe68 seems to occupy a more solvent-exposed position in the solution structure, although its conformation is not well defined by the NMR data.

In order to form a tight turn in the EF loop, Pro71 (EF3) adopts a *cis* conformation. The homologous proline residue in N-SH2 also adopts the *cis* conformation, as shown in the crystal structures. In the NMR study of C-SH2 no resonances for this residue could be found, probably due to exchange broadening. As described above, Pro71 (EF3) makes an important crystal contact that may serve to freeze out the exchange processes observed in solution. However, the *cis* conformation also seems to be important for positioning Phe68 (βE4) and for allowing O^{δ} of Asn73 (βF2) to form a hydrogen bond to N^{δ} of Asn60 (βD′3). Recent evidence implies that the entire EF region may be undergoing slow, concerted motions in solution (Kristensen *et al.*, unpublished results).

Superposition of the crystal structures of C-SH2 and N-SH2 shows that Tyr72 (βFI) in C-SH2 is an insertion rather than a substitution (see Figure 4(b)). It is possible that this residue prevents the binding of bulky side-chains at the $pY+6$ position, as seen in the N-SH2/pY-c-kit structure (data not shown). However, since its position in the solution structure is also not precisely determined, this conjecture awaits experimental verification.

BG loop

In the crystal structure of C-SH2, N^{ε} of His93 (BG6) at the tip of the BG loop forms a hydrogen bond to the side-chain hydroxyl of Tyr85 (αB9). In N-SH2, residue BG6 is Tyr95. Upon superposition of the backbone structures of C-SH2 and N-SH2 bound to pY-PDGFR, residues BG6 and αB9 in both structures also superimpose (see Figure 4(b)). This particular interaction is only seen in the liganded N-SH2 structures. In unliganded N-SH2, residue BG6 is exposed to solvent and αB9 makes a hydrogen bond to BG5 (Gln94) instead. Once again, the crystal structure of C-SH2 looks more like the ligand-bound structures in this respect. However, in the solution structure of C-SH2 complexed to the pY740 peptide, His93 (BG6) is shifted away from the core of the protein. In fact, superposition of the crystal structure and the solution structure of the liganded C-SH2 results in steric clash between His93 (BG6) of the crystal structure and the peptide backbone. Clearly a crystal structure of the ligand-bound C-SH2 is required to resolve this difference.

Conclusions

The crystal structure of C-SH2 is unique in that it has characteristics of both a ligand-free and a ligand-bound SH2 domain. This is understandable for the residues that contribute to the pY binding pocket, as the interaction with Asp2 of a neighbouring molecule clearly mimics that of the phosphate moiety of the natural ligand. Because of this interesting interaction, and probably also because of other crystal contacts, some regions in the protein adopt specific conformations not observed in the solution structure. This structure both corroborates the recent finding that non-phosphate-containing ligands can be potent inhibitors of pY binding of SH2 domains *in vitro* and *in vivo* (Yao *et al.*, 1999), and extends them to define the particular intermolecular interactions. It is somewhat surprising that the side-chain of an aspartate residue can productively occupy the pocket designed to accommodate the much larger phosphotyrosine. It is apparent that SH2 domains have at least some flexibility in adapting to particular ligands. However, it should be said that in solution the aspartate residue is expected to have significantly lower binding affinity than phenyl phosphate. Nonetheless, given the principle of SAR-by-NMR (Hajduk *et al.*, 1997), it is expected that

studies with mono-carboxylic, non-aromatic compounds may lead to productive new paths in the discovery and development of inhibitors of SH2 domain binding to phosphotyrosine ligands.

Protein Data Bank accession number

Structure factors and atomic co-ordinates have been deposited with the PDB (accession number 1QAD).

Acknowledgements

The authors thank Anastassis Perrakis and Garib Murshudov for helpful discussions, and Dr R.T. Nolte for providing the co-ordinates of the N-SH2 domain structures.

References

Abola, E. E., Sussman, J. L., Prilusky, J. & Manning, N. O. (1997). Protein data bank archives of three-dimensional macromolecular structures. *Methods Enzymol.* **277**, 556-571.

Breeze, A. L., Kara, B. V., Barratt, D. G., Anderson, M., Smith, J. C., Luke, R. W., Best, J. R. & Cartlidge, S. A. (1996). Structure of a specific peptide complex of the carboxy-terminal SH2 domain from the p85α subunit of phosphatidylinositol 3-kinase. *EMBO J.* **15**, 3579-3589.

Brünger, A. T. (1992). *X-PLOR Version 3.1. A System for X-ray Crystallography and NMR*, Yale University Press, New Haven, CT.

Collaborative Computational Project Number 4 (1994). The CCP4 suite: programs for protein crystallography. *Acta Crystallog. sect. D,* **50**, 760-763.

Dhand, R., Hara, K., Hiles, I., Bax, B., Gout, I., Panayotou, G. & Waterfield, M. D. (1994). PI 3-kinase: structural and functional analysis of intersubunit interactions. *EMBO J.* **13**, 511-521.

Eck, M. J., Shoelson, S. E. & Harrison, S. C. (1993). Recognition of a high-affinity phosphotyrosyl peptide by the Src homology-2 domain of p561ck. *Nature,* **362**, 87-91.

Evans, P. R. (1997). Scala. *Joint CCP4 and ESF-EACBM Newsletter,* **33**, 22-24.

Fu, J-M. & Castelhano, A. L. (1998). Design and synthesis of a pyridone-based phosphotyrosine mimetic. *Bioorg. Med. Chem. Letters,* **18**, 2813-2816.

Groves, M. R., Yao, Z. J., Roller, P. P., Burke, T. R., Jr & Barford, D. (1998). Structural basis for inhibition of the protein tyrosine phosphatase 1B by phosphotyrosine peptide mimetics. *Biochemistry,* **37**, 17773-17783.

Hajduk, P. J., Meadows, R. P. & Fesik, S. W. (1997). Discovering high-affinity ligands for proteins. *Science,* **278**, 497-499.

Hatada, M. H., Xiaode, L., Laird, E. R., Green, J., Morgenstern, J. P., Lou, M., Marr, C. S., Phillips, T. B., Ram, M. K., Theriault, K., Zoller, M. J. & Karas, J. L. (1995). Molecular basis for interaction of the protein tyrosine kinase ZAP-70 with the T-cell receptor. *Nature,* **377**, 32-38.

Hooft, R. W., Vriend, G., Sander, C. & Abola, E. E. (1996). Errors in protein structures. *Nature,* **381**, 272.

Jones, T. A., Zoti, J. Y., Cowan, S. W. & Kjeldgaard, M. (1991). Improved methods for binding protein models in electron density maps and the location of errors in these models. *Acta Crystallog. sect. A,* **47**, 110-119.

Kashishian, A., Kazlauskas, A. & Cooper, J. A. (1992). Phosphorylation sites in the PDGF receptor with different specificities for binding GAP and PI3 kinase in vivo. *EMBO J.* **11**, 1373-1382.

Mikol, V., Baumann, G., Keller, T. H., Manning, U. & Zurini, M. G. (1995). The crystal structures of the SH2 domain of p561ck complexed with two phosphonopeptides suggest a gated peptide binding site. *J. Mol. Biol.* **246**, 344-355.

Murshudov, G. N., Vagin, A. A. & Dodson, E. J. (1997). Refinement of macromolecular structures by the maximum-likelihood method. *Acta Crystallog. sect. D,* **53**, 240-255.

Nolte, R. T., Eck, M. J., Schlessinger, J., Shoelson, S. E. & Harrison, S. C. (1996). Crystal structure of the PI-3-kinase p85α amino-terminal SH2 domain and its phosphopeptide complexes. *Nature Struct. Biol.* **3**, 364-374.

Otsu, M., Hiles, L., Gout, I., Fry, M. J., Ruizlarrea, F., Panayotou, G., Thompson, A., Dhand, R., Hsuan, J., Totty, N., Smith, A. D., Morgan, S. J., Courtneidge, S. A., Parker, P. J. & Waterfield, M. D. (1991). Characterisation of two 85 kDa proteins that associate with receptor tyrosine kinases, middle-T/pp60c-src complexes, and PI 3-kinase. *Cell,* **65**, 91-104.

Panayotou, G., Gish, G., Truong, O., Gout, L., Dhand, R., Fry, M. J., Hiles, L., Pawson, T. & Waterfield, M. D. (1993). Interactions between SH2 domains and tyrosine-phosphorylated platelet-derived growth factor β-receptor sequences: analysis of kinetic parameters by a novel biosensor-based approach. *Mol. Cell. Biol.* **13**, 3567-3576.

Pascal, S. M., Singer, A. U., Gish, G., Yamazaki, T., Shoelson, S. E., Pawson, T., Kay, L. E. & Forman, Kay J. D. (1994). Nuclear magnetic resonance structure of an SH2 domain of phospholipase C-γl complexed with a high affinity binding peptide. *Cell,* **77**, 461-472.

Perrakis, A., Morris, M. & Lainzin, V. S. (1999). Automated protein model building combined with iterative structure refinement. *Nature Struct. Biol.* **6**, 458-463.

Rahuel, J., Gay, B., Erdmann, D., Strauss, A., Garciaecheverria, C., Furet, P. & Grutter, M. G. (1996). Structural basis for specificity of Grb2-SH2 revealed by a novel ligand-binding mode. *Nature Struct. Biol.* **3**, 586-589.

Rordorf-Nikolic, T., Van Horn, D. J., Chen, D., White, M. F. & Backer, J. M. (1995). Regulation of phosphatidylinositol 3-kinase by tyrosyl phosphoproteins: full activation requires occupancy of both SH2 domains in the 85-kDa regulatory subunit. *J. Biol. Chem.* **270**, 3662-3666.

Siegal, G., Davis, B., Kristensen, S. M., Sankar, A., Linacre, J., Stein, R. C., Panayotou, G., Waterfield, M. D. & Driscoll, P. C. (1998). Solution structure of the C-terminal SH2 domain of the p85α regulatory subunit phosphoinositide 3-kinase. *J. Mol. Biol.* **276**, 461-478.

Songyang, Z., Shoelson, S. E., Chaushuri, M., Gish, G., Pawson, T., Haser, W., King, F., Roberts, T., Ratnofsky, S., Lechleider, R. J., Neel, B. G., Birge, R. B., Fajardo, J. E., Chou, M. M., Hanafusa, H.,

et al. (1993). SH2 domains recognise specific phosphopeptide sequences. *Cell,* **72**, 767-778.
Songyang, Z., Gish, G., Mbamalu, G., Pawson, T. & Cantley, L. C. (1995). A single point mutation switches the specificity of group-III Src homology SH2 domains to that of group-I SH2 domains. *J. Biol. Chem.* **270**, 26029-26032.
Toker, A. & Cantley, L. C. (1997). Signalling through the lipid products of phosphoinositide-3-OH kinase. *Nature,* **387**, 673-676.
Vanhaesebroeck, B., Leevers, S. J., Panayotou, G. & Waterfield, M. D. (1997). Phosphoinositide 3-kinases: a conserved family of signal transducers. *Trends Biochem. Sci.* **22**, 267-272.
Waksman, G., Shoelson, S. E., Pant, N., Cowburn, D. & Kuriyan, J. (1993). Binding of a high-affinity phosphotyrosyl peptide to the Src SH2 domain: crystal structures of the complexed and peptide-free forms. *Cell,* **72**, 779-790.
Yao, Z. J., King, C. R., Cao, T., Kelley, J., Milne, G. W., Voigt, J. H. & Burke, T. R., Jr (1999). Potent inhibition of Grb2 SH2 domain binding by non-phosphate-containing ligands. *J. Med. Chem.* **42**, 25-35.
Zhang, W., Smithgall, T. E. & Gmeiner, W. H. (1997). Sequential assignment and secondary structure determination for the Src homology 2 domain of hematopoietic cellular kinase. *FEBS Letters,* **406**, 131-135.

Edited by I. A. Wilson

(Received 12 May 1999; received in revised form 4 August 1999; accepted 6 August 1999)

Update

Journal of Molecular Biology
Volume 294, Issue 3, 3 December 1999, Page 825

DOI: https://doi.org/10.1006/jmbi.1999.3337

JMB

ERRATUM

Crystal Structure of the C-Terminal SH2 Domain of the p85α Regulatory Subunit of Phosphoinositide 3-Kinase: An SH2 Domain Mimicking its Own Substrate

F. J. Hoedemaeker, G Siegal, S. M. Roe, P. C. Driscoll and J. P. Abrahams

J. *Mol. Biol.* (1999) 292, 763–770

The legends to Figure 4(b) and Figure 4(c) were switched and should have appeared as follows:

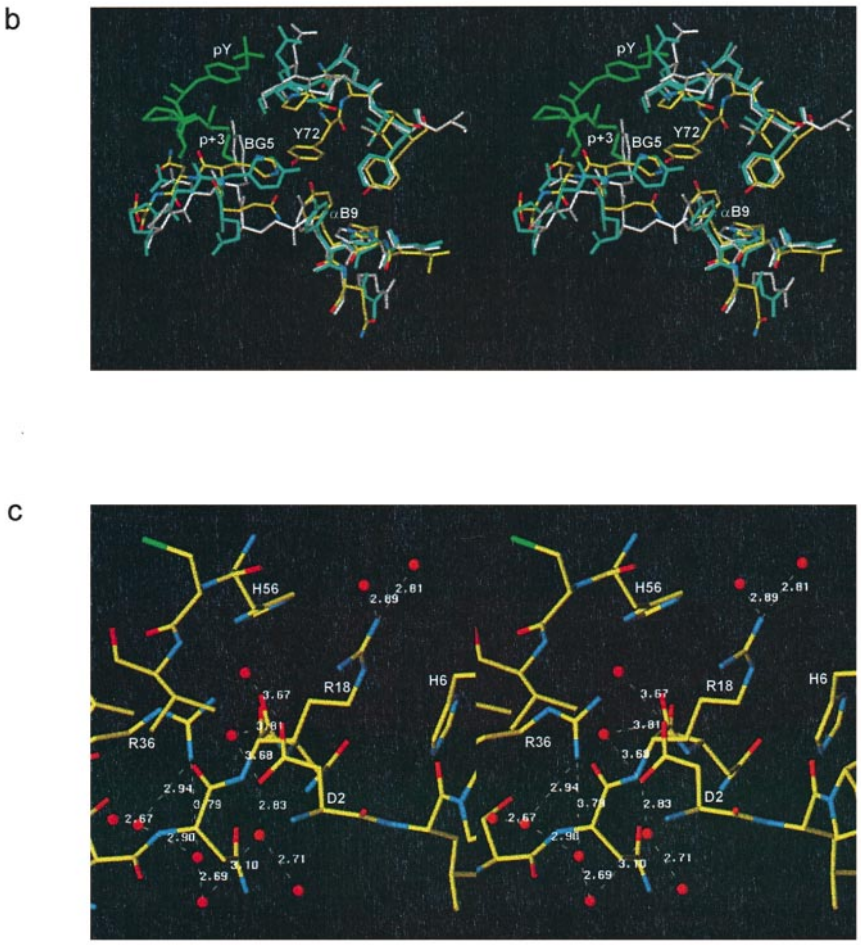

Figure 4. Detailed (divergent) stereo images. (a) The binding of Asp2 of a crystallographic neighbour to the active-site residues Arg18 (αA2) and Arg36 (βB5). Pro71 of a third SH2 molecule is also involved in this crystal contact. (b) The binding pocket for the ligand residue Met pY + 3. Ligand-free N-SH2 is shown in grey, N-SH2 liganded to pY-PDGFR is shown in blue (with part of the pY peptide in green), and C-SH2 is shown in CPK colouring. His BG6 is in a position comparable with liganded N-SH2 and not with unliganded N-SH2, making a hydrogen bond to Tyr αB9. The insertion of Tyr72 in the sequence is clearly visible. (c) Water structure surrounding the binding pocket: a network of well-ordered water molecules forms one side of the binding pocket.

0022-2836/99/480825–1 $30.00/0